Eur Biophys J (2008) 37:591–602
DOI 10.1007/s00249-008-0274-3

ORIGINAL PAPER

The dynamical transition of proteins, concepts and misconceptions

Wolfgang Doster

Received: 14 October 2007 / Revised: 10 January 2008 / Accepted: 17 January 2008 / Published online: 13 February 2008

Abstract The dynamics of hydrated proteins and of protein crystals can be studied within a wide temperature range, since the water of hydration does not crystallize at low temperature. Instead it turns into an amorphous glassy state below 200 K. Extending the temperature range facilitates the spectral separation of different molecular processes. The conformational motions of proteins show an abrupt enhancement near 180 K, which has been called a "dynamical transition". In this contribution various aspects of the transition are critically reviewed: the role of the instrumental resolution function in extracting displacements from neutron elastic scattering data and the question of the appropriate dynamic model, discrete transitions between states of different energy versus continuous diffusion inside a harmonic well, are discussed. A decomposition of the transition involving two motional components is performed: rotational transitions of methyl groups and small scale librations of side-chains, induced by water at the protein surface. Both processes create an enhancement of the observed amplitude. The onset occurs, when their time scale becomes compatible with the resolution of the spectrometer. The reorientational rate of hydration water follows a super-Arrhenius temperature dependence, a characteristic feature of a dynamical transition. It occurs only with hydrated proteins, while the torsional motion of methyl groups takes place also in the dehydrated or solvent-vitrified system. Finally, the role of fast hydrogen bond fluctuations contributing to the amplitude enhancement is discussed.

Keywords Protein dynamics · Neutron scattering · Dynamical transition · Glass transition · Protein hydration · Myoglobin · Lysozyme

Advanced neutron scattering and complementary techniques to study biological systems. Contributions from the meetings, "Neutrons in Biology", STFC Rutherford Appleton Laboratory, Didcot, UK, 11–13 July and "Proteins At Work 2007", Perugia, Italy, 28–30 May 2007.

W. Doster (✉)
Physics Department E13, Technical University Munich,
85748 Garching, Germany
e-mail: wdoster@ph.tum.de

Introduction: how many dynamical transitions?

The abrupt deviation of structural mean square displacements in proteins from a linear temperature dependence is commonly assigned to a dynamical transition. Often it is unclear, whether the apparent onset of non-vibrational protein motions reflects the properties of the spectrometer or whether there is a physical transition in the dynamic structure factor. The two basic mechanisms inducing an abrupt enhancement of the recorded displacements are the exponential increase in motional amplitude due to states of different energy and the exponential (or super-exponential) increase in rate with temperature. Unfortunately both types of processes interfere near 200 K with hydrated proteins in elastic neutron scattering experiments and Mössbauer spectroscopy. This has caused considerable confusion. The term "dynamical transition" was reserved in 1989 (Doster et al. 1989, 1986, 1990; Lichtengegger et al. 1999) to protein motions, which are coupled to the kinetic glass transition of the solvent near the protein surface. The low-temperature onset below 180 K was assigned originally to torsional motions of side-chains between states of different energy (Doster et al. 1989). Below it is shown that the correct assignment involves rotational transitions of methyl groups between nearly isoenergetic states.

The main idea of including the subzero temperature range, was to separate the variety of molecular processes according to their time-scale. The displacements $\langle \Delta x^2 \rangle$ in such experiments are often derived from elastic scattering profiles $I_{el}(Q)$ versus momentum exchange Q using a Gaussian model:

$$I_{el}(Q) = I_{el}^0 \cdot \exp\left(-Q^2 \langle \Delta x^2 \rangle\right). \quad (1)$$

Only neutrons scattered with zero energy exchange are counted with finite, but fixed energy resolution. This implies, that only processes which are fast enough to be resolved by the spectrometer contribute to the loss in the elastic scattering intensity. The resulting displacements thus carry the time-tag of the spectrometer. A combination of different neutron spectrometers covering a wider time window can further extend the potential to identify particular molecular motions in proteins. Moreover the incoherent scattering profile versus scattering angle is related to the spatial displacement distribution of the molecular process. Thus, the wide Q-range (up to 5 Å^{-1}) of the back-scattering spectrometer IN13 at the ILL in Grenoble is crucial to achieve molecular assignements based on spatial characteristics (Doster et al. 1989; Doster and Settles 2005; Doster 2006). Mössbauer spectroscopy provides an even larger Q-value of 7.31 Å^{-1}. This method is thus sensitive to small scale displacements at a much higher resolution than what is achieved with neutron scattering. A similar dynamical transition was observed with the heme iron as monitor in myoglobin crystals (Parak and Formanek 1971; Parak et al. 1981; Parak and Knapp 1984). To study hydrated proteins at full hydration, but below $h = 0.4$ g water/g protein, instead of solutions is useful for the following reasons:

Hydration water does not freeze at subzero temperatures, instead it vitrifies forming a glassy state (Doster et al. 1986; Demmel et al. 1997). Ice formation would freeze-dry the protein, the pH and salt composition of the resulting non-freezable solvent fraction can differ drastically from the liquid bulk, which may denature the protein (Doster et al. 1986; Sartor et al. 1994). The melting of bulk water in such samples becomes apparent through an abrupt increase in the molecular displacements near 273 K related to the onset of D_2O- and protein diffusion (Ferrand et al. 1993; Zaccai 2000). Depending on the experimental history, also cubic ice is formed, which melts at 210 K and crystallizes again into a hexagonal phase (Sartor et al. 1994). An equilibrium phase transition differs from a dynamical transition, which is a kinetic phenomenon. The amount of non-freezable water at full protein hydration (0.4 g/g) is quite similar to what is generally found in protein crystals. Proteins in crystals often are biologically active. At such high concentrations, rotational diffusion and center of mass diffusion are suppressed due to mutual hindrance. The neutron scattering spectrum is thus dominated by protein-internal motions and incoherent scattering from the protein. The contribution of the deuterated solvent to the spectrum is often below 5% and can be neglected.

In the neutron scattering study of dry and hydrated myoglobin in 1989 (Doster et al. 1989) two transition temperatures at 180 and 240 K were identified and were assigned to two different molecular processes: torsional jumps of side-chains between states of different energy and water-induced collective motions. The latter were not observed in the dehydrated state. The onset of collective motion at 240 K was attributed to a kinetic melting of glassy water in the hydration shell (Doster et al. 1989, 1986; Demmel et al. 1997). Thus only the second onset was assigned to a "dynamical transition" in analogy to the glass transition. The first onset at 180 K was interpreted in terms of a glass-transition precursor, being mediated by fast hydrogen-bond fluctuations between states of different energy. Both processes, termed α and β, in the glass literature (Götze and Sjögren 2005) play a role in hydrated proteins. However, recently it was shown, that a third process, the rotational transitions of side chains, unrelated to the glass transition, interferes with the onset at 180 K (Doster and Settles 2005; Doster 2006; Roh et al. 2005). The dynamical transition proved to be a generic feature of hydrated proteins and not just of myoglobin. However, any anharmonic onset in the displacements, irrespective of its origin, was now called a "dynamical transition" (Smith 1991; Fitter et al. 1997; Zaccai 2000; Gabel et al. 2002). The two-component onset in the displacements and the important role of hydration water in the transition were rediscovered several times in the literature (Reat et al. 1997; Tournier and Smith 2003; Roh et al. 2005). In principle, two types of processes can give rise to enhanced displacements above a specific temperature: (a) the amplitude of molecular motions increases exponentially with temperature due to occupation of states with higher energy and (b) the characteristic time of a molecular process enters the time window accessible to the spectrometer. The latter can be identified by varying the spectral resolution. In fact at least three different types of molecular motions contribute to the spectrum near 200 K. A simple decomposition based on elastic scattering data is thus difficult. In the following we summarize the analytical tools and their application to unravel the motions contributing to the onset of diffusive displacements.

Data analysis

The role of instrumental resolution

The elastic scattering intensity measured at zero energy exchange ($\omega = 0$), is a complex quantity, which depends

on the width of instrumental resolution function $\Delta\omega$, the incoherent elastic scattering fraction, EISF (Q), and the time constant τ_c of the observed dynamic process: I_{el} (Q,$\Delta\omega$) is defined by the convolution of the resolution function of the spectrometer R (Q,ω,$\Delta\omega$) and the dynamical structure factor of the sample S (Q,ω) at $\omega = 0$ (Doster and Settles 1998):

$$I_{\mathrm{el}}(Q,\Delta\omega) = \int_{-\infty}^{\infty} R(Q,\omega',\Delta\omega) * S(Q,\omega')\mathrm{d}\omega'. \tag{2}$$

Separating relaxational from vibrational components of the spectrum yields for the elastic scattering function:

$$I_{\mathrm{el}}(Q)/I_{\mathrm{el}}(Q=0) = \mathrm{e}^{-2W}[\mathrm{EISF}(Q) + (1-\mathrm{EISF}(Q)) \cdot R(\Delta\omega,\tau_c)] \tag{3}$$

$\mathrm{e}^{-2W(Q)}$ denotes the vibrational Debye–Waller factor. A Gaussian resolution function of width $\sigma = \Delta\omega = 1/\tau_{\mathrm{res}}$, applies to time-of-flight and back-scattering spectroscopy. For a process exhibiting a Lorentzian spectrum (2) leads to the following resolution correction R_L of the elastic intensity in (3):

$$R_L(\Delta\omega,\tau_c) = \frac{2}{(2\pi)^{3/2}} \int_{-\infty}^{\infty} \exp(-\frac{\omega^2}{2\Delta\omega^2}) \frac{\tau_c}{(1+\omega^2\tau_c^2)}\mathrm{d}\omega \tag{4}$$

the integral can be written in a closed form (Doster et al. 2001, 2003):

$$R_L(\tau_{\mathrm{res}}/\tau_c) = \mathrm{erfc}\left(\frac{\tau_{\mathrm{res}}/\tau_c}{\sqrt{2}}\right) \cdot \exp\left(\frac{\tau_{\mathrm{res}}^2/\tau_c^2}{2}\right). \tag{5}$$

Here erfc(x) is the complementary error function. Equation 5 was first applied by Doster and Settles (1998), and Doster et al. (2001, 2003) to analyse the elastic intensity as function of the instrumental resolution. With this method one derives the intermediate scattering function in the time domain from variable resolution experiments in the frequency domain. The technique is called "elastic resolution spectroscopy" and is can cope with weakyl scattering samples, where only the elastic intenstiy can be evaluated above the noise level. The effect of a finite resolution on the elastic scattering intensity was also considered in Becker and Smith (2003), Becker et al. (2004) and Gabel (2005).

Figure 1 shows the apparent mean square displacements of a resolution-limited process, assuming a variable time window $\tau_{\mathrm{res}} = 1/\Delta\omega$ of the spectrometer for various fixed values of τ_c. A small τ_{res} implies a large spectral width in frequency space and thus a low resolution. Increasing the time window and thus τ_{res} enhances the instrumental

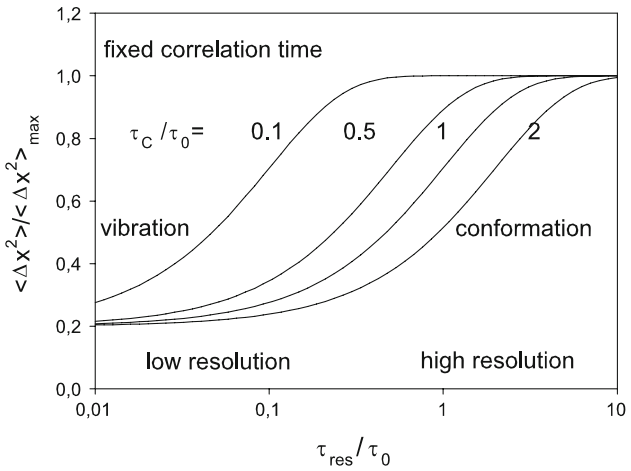

Fig. 1 Apparent mean square displacements of a process with fixed correlation time τ_c depending on the instrumental time window τ_{res}. τ_0 denotes a reference time

resolution. At $\tau_{\mathrm{res}} \approx 0{,}2\cdot\tau_c$, the onset occurs. The instrumental resolution can be varied within a wide range using time-of-flight spectrometers by changing either the wavelength or the chopper speed. R_L is small but not zero for processes, which are much faster than those defined by the instrumental width, $1/\tau_c \gg \Delta\omega$. Only in this case one may approximate the elastic intensity by $I_{\mathrm{el}}(\mathrm{Q}) \approx \mathrm{e}^{-2W}$. EISF($Q$).

The total displacement is composed of a vibrational and a configurational part:

$$\langle\Delta x^2\rangle = \langle\Delta x_{\mathrm{vib}}^2\rangle + \langle\Delta x_{\mathrm{conf}}^2\rangle. \tag{6}$$

The vibrational displacements increase linearly with temperature, while the configurational displacement can increase exponentially for the reasons mentioned above. If the instrumental resolution is the limiting factor one can expand (3) at low Q according to:

$$\langle\Delta x^2\rangle = \langle\Delta x_{\mathrm{vib}}^2\rangle + \langle\Delta x_{\mathrm{conf}}^2\rangle(1 - R_L(\tau_{\mathrm{res}}/\tau_c)). \tag{7}$$

A dynamical transition is a kinetic feature caused by a relaxation rate with a super-Arrhenius temperature dependence. A conventional molecular process with Arrhenius behaviour would not give rise to a dynamical transition, but would still cause a nonlinear enhancement in the displacements above a certain temperature. Figure 2 compares the effect of different rate laws, Arrhenius and super-Arrhenius, on the onset of anharmonic motions. The super-Arrhenius onset is more abrupt due to strong variation of $\tau_c(T)$ Various rate laws have been proposed to characterize super-Arrhenius behaviour.

The Vogel–Fulcher law is often used to describe the molecular relaxation times near a glass transition:

$$\tau_c = \tau_0 \cdot \exp(A^*/(T - T_0)) \tag{8}$$

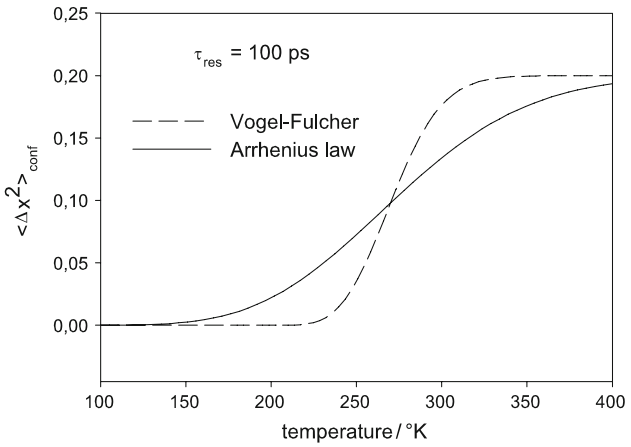

Fig. 2 Resolution-limited mean square displacements observed with a resolution time window of $\tau_{res} \approx$ 100 ps versus the temperature for processes with rates following either an Arrhenius law (*solid lines*) or a super-Arrhenius temperature dependence (*dashed lines*). Parameters: $\Delta G^*/R$=1,350 K, τ_0 = 1 ps, A^* = 500 K and T_0 = 170 K

$A^* = \Delta G^*/R$ is related to the high-temperature activation free energy ΔG^*. When the critical temperature T_0 is approached from above, non-Arrhenius behaviour results. Activated transitions of side-chains follow the Arrhenius law, while fluctuations coupled to the solvent exhibit deviations, in particular near a glass transition.

Displacements derived in the time- or frequency-domain: the factor of two

Considerable confusion exists in the literature on how to extract mean square displacements from elastic scattering data. From the arguments given above it is obvious, that the observed displacements refer to a maximum time scale, limited by the resolution of the spectrometer. Usually the peak intensity of the spectrum at $\omega = 0$, the elastic intensity $I_{el}(Q)$, is evaluated assuming the Gauss approximation (Roh et al. 2005; Zaccai 2000):

$$I_{el}(Q)/I_{el}(Q=0) \approx e^{-\frac{1}{3}Q^2\langle\Delta\vec{r}^2\rangle} = e^{-Q^2\langle\Delta x^2\rangle}. \quad (9)$$

Here $\langle\Delta\vec{r}^2\rangle$ denotes the three-dimensional, powder-averaged squared displacement vector. For isotropic samples the squared displacements projected to one dimension are then given by: $\langle\Delta\vec{r}^2\rangle = 3\ \langle\Delta x^2\rangle$. Sometimes the displacements are denoted by "u", leaving open whether one- or three-dimensional motion is implied (Fitter et al. 1997; Daniel Smith et al. 1998; Daniel et al. 1999; Tsai et al. 2000; Gabel et al. 2002; Russo et al. 2002; Tournier and Smith 2003; Paciaroni et al. 2006; Tehei et al. 2006b). The factor 1/3 in the exponent of (9) (Doster et al. 1989; Doster and Settles 2005; Reat et al. 2000; Bicout and Zaccai 2001), is often replaced by 1/6 without explanation (Gabel et al. 2002; Becker and Smith 2003; Hayward et al. 2003; Tournier et al. 2003, 2003; Tournier and Smith 2003; Becker et al. 2004; Nakagawa et al. 2004; Roh et al. 2005; Gabel 2005; Tehei et al. 2005, 2006a, b; Kurkal et al. 2005; Serdyuk et al. 2007), which is incorrect. Moreover, the elastic scattering profiles of proteins are generally not Gaussian as was first demonstrated in 1989 (Doster et al. 1989). This originates from a dynamic heterogeneity (at least two processes) in combination with an intrinsic non-Gaussian displacement distribution due to side-chain rotation (Doster and Settles 2005). Thus (9) applies only in the limit of low Q-values. Sometimes average values based on fits covering a much wider Q-range are presented (Ferrand et al. 1993). To spot the origin of the discrepancy by a factor of two from the displacements of (9), we start with the definition of the incoherent intermediate scattering function $I(\vec{Q},t)$, which is the self-correlation function of the phase factors:

$$I(\vec{Q},t) = \left\langle e^{i\vec{Q}\vec{r}(0)} \cdot e^{-i\vec{Q}\vec{r}(t)} \right\rangle. \quad (10)$$

The elastic fraction is defined as the long-time limit of the intermediate scattering function:

$$\mathrm{EISF}(Q) = I(Q, t\to\infty) \approx I_{el}(Q, \tau_{res}\to\infty)/I_{el}(Q=0). \quad (11)$$

In this limit the phase factors are decorrelated, and their average can be factorized assuming a stationary state:

$$I(\vec{Q},t) = \left\langle e^{i\vec{Q}\vec{r}(0)} \right\rangle \left\langle e^{-i\vec{Q}\vec{r}(t\to\infty)} \right\rangle = \left| e^{i\vec{Q}\vec{r}(0)} \right|^2. \quad (12)$$

Spezializing to a Gauss distribution and one dimension Q = Q_x, we can write (12) as:

$$\mathrm{EISF}(Q) = \left[\frac{1}{\sqrt{2\pi\langle\Delta x^2\rangle}} \int dx \cdot e^{-\frac{x^2}{2\langle\Delta x^2\rangle}} e^{-iQx} \right]^2 = e^{-Q^2\langle\Delta x^2\rangle} \quad (13)$$

which yields (9) since $\langle\Delta x^2\rangle = \langle\Delta r^2\rangle/3$ in isotropic samples.

One can calculate the displacements from (10) in a slightly different manner: We write $\vec{r}(t) = \vec{r}(0) + \Delta\vec{r}(t)$ and perform the isotropic Gauss-average:

$$I(\vec{Q},t) = \left\langle e^{-i\vec{Q}\Delta\vec{r}(t)} \right\rangle = I(Q,t) = e^{-\frac{1}{6}Q^2\langle\Delta r^2(t)\rangle} = e^{-\frac{1}{2}Q^2\langle\Delta x^2(t)\rangle}. \quad (14)$$

Note that the phase factor average involving the time-resolved displacements is not squared. Comparing both displacements in the long time limit, they differ by a factor of two:

$$\langle\Delta x^2(t\to\infty)\rangle = 2\langle\Delta x^2\rangle_{\mathrm{EISF}}. \quad (15)$$

To conclude, the squared average displacement determined in the time domain is twice as large as the corresponding

squared displacement derived in the frequency domain at the same resolution. This discrepancy is the origin of the confusion mentioned above.

Features of the double-well model

The two-state system has often been employed as a model of the dynamical transition. It is a discontinuous model in contrast to the "force constant model" of Bicout and Zaccai (2001), which assumes continuous motions within a harmonic potential. Below we ask, whether it makes sense to approximate the non-linear region by straight lines based on a two-state analysis. The discrete model also serves to illustrate the two basic mechanisms of the anharmonic onset in the apparent displacements: (1) a temperature-induced shift between the population of two states of different free energy ΔG or (2) a temperature-induced enhancement of the transition rate between the wells with respect to the frequency resolution of the spectrometer. The population of the excited state in the former case will thus increase with temperature. The relaxation rate of the system is determined by the combination of the up- and down-transition rate between the ground and the excited state. If the barrier in the excited state is small, a rate coefficient results, which is nearly independent of the temperature. This type of model, initially assumed by Doster et al. (1989), applies to transitions between open and closed states of hydrogen bonds in water or between water and a protein surface (Doster and Settles 1998, 2005), but not to methyl group rotation. Because the correlation time of H-bond fluctuations ranges near 1 ps (Doster and Settles 2005), one can safely ignore the effects of the instrumental resolution function. Only the free energy difference ΔG between open and close states matters.

Assuming a maximum squared average displacement of $\langle \Delta x^2_{\mathrm{DW}} \rangle$ one has for the apparent conformational displacements (Doster et al. 1989):

$$\langle \Delta x^2_{\mathrm{conf}} \rangle = \langle \Delta x^2_{\mathrm{DW}} \rangle \cdot \frac{\mathrm{e}^{-\Delta G/RT}}{(1+\mathrm{e}^{-\Delta G/RT})^2} \approx \langle \Delta x^2_{\mathrm{DW}} \rangle \cdot \mathrm{e}^{-\Delta G/RT} \tag{16}$$

for $\Delta G \gg$ RT. This leads to a sharp exponential onset, independent of the instrumental resolution, whenever this value becomes comparable in magnitude to the vibrational displacements $\langle \Delta x^2_{\mathrm{vib}}(T) \rangle$. Bicout and Zaccai propose to approximate the combined temperature dependence by two fixed slopes, which they attribute to effective force constants (Bicout and Zaccai 2001). The corresponding slope of the conformational component far below saturation is approximately given by:

$$\frac{\mathrm{d}\langle \Delta x^2_{\mathrm{conf}} \rangle}{\mathrm{d}T} \approx \langle \Delta x^2_{\mathrm{DW}} \rangle \cdot \frac{\Delta G}{RT^2} \cdot \mathrm{e}^{-\Delta G/RT}. \tag{17}$$

The result is shown in Fig. 3. The apparent force constant in a discrete jump model is thus never constant, it increases strongly with temperature up to $k_BT/\Delta G \approx 0.5$ and vanishes at high temperatures due to population saturation. A temperature-independend slope requires the assumption of a pseudo-harmonic potential, which is a very special assumption. In the symmetric two-well potential one has $\Delta G = 0$). The anharmonic onset in this case follows from (7), where τ_c denotes the correlation time of the transition between the wells and τ_{res} defines the time window of the spectrometer. The nonharmonic onset occurs when the conformational displacements are resolved, $\tau_c \approx 5\ \tau_{\mathrm{res}}$, as shown in Fig. 1. To prove the point we assume for simplicity:

$$R(\tau, \tau_{\mathrm{res}}) \approx \mathrm{e}^{-\tau_{\mathrm{res}}/\tau_c(T)} \tag{18}$$

and the Arrhenius law:

$$\tau_c = \tau_0 \cdot \mathrm{e}^{\Delta G^*/k_BT} \tag{19}$$

ΔG^* denotes the activation free energy of the barrier separating the the two states.

For the temperature slope of the displacements one obtains in the limit $\Delta G^* \gg k_BT$:

$$\frac{\mathrm{d}\langle \Delta x^2_{\mathrm{conf}} \rangle}{\mathrm{d}T} \approx \langle \Delta x^2_{\mathrm{DW}} \rangle \cdot \frac{\Delta G^*}{RT^2} \cdot \frac{\tau_{\mathrm{res}}}{\tau_c(T)} \mathrm{e}^{-\tau_{\mathrm{res}}/\tau_c(T)}. \tag{20}$$

Again the slope or the apparent force constant depends strongly on the temperature, the activation energy and the time window of the spectrometer. It vanishes in both limits of short and long resolution times τ_{res} with respect to $\tau_c(T)$. In addition the energy gap is replaced by the activation

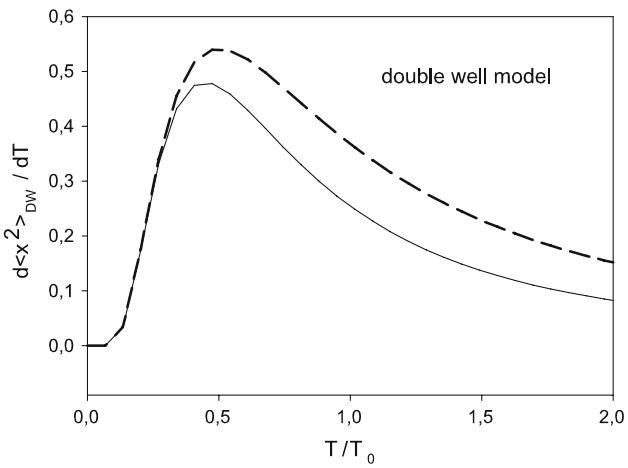

Fig. 3 Normalized temperature slope (reciprocal force constant) of mean square displacements according to the two-well model, *full line*: strongly asymmetric case, population dominated: $T_0 = \Delta G/R$, *dashed line*: symmetric case (resolution dominated) with $T_0 = \Delta G^*/R$

energy ΔG^*. The apparent resilence reflects in one case an energy gap or, alternatively, an activation energy. As was noted alread in early work (Doster et al. 1989), a double-well model, symmetric or asymmetric, does not account for the second onset induced by collective, water-coupled protein motions (Doster and Settles 2005; Doster 2006). Here an overdamped harmonic oscillator with Gaussian displacements is more appropriate (Doster 2005). As will be discussed below, the onset recorded with hydrated proteins employing the back-scattering spectrometer IN13 are mostly resolution controlled, suggesting a symmetric model. Moreover an Arrhenius law fails to describe the temperature dependence of water-reorientation near the protein surface at low temperatures. It was demonstrated that the structural relaxation relaxation time of protein residues near the protein surface vary in proportion to the local solvent viscosity (Lichtengegger et al. 1999): $\tau_c \propto \eta$. For the apparent displacements, observed with a given resolution time window τ_{res}, one obtains from (7, 18, 19) near the onset temperature $\tau_{\text{res}}/\tau_c \approx 0.2$:

$$\left\langle \Delta x^2_{\text{conf}} \right\rangle = C\tau_{\text{res}}/\eta \tag{21}$$

which is the result expected for a Brownian particle moving in a solvent with viscosity η. For solvent-coupled protein processes it is the local viscosity near the protein surface and not the bulk viscosity which matter (Lichtengegger et al. 1999). In their neutron scattering data analysis of proteins in various solvents, Magazou et al. (2004; Cornicchi et al. 2005) use a different phenomenological relation, which was orignally suggested by Buchenau and Zorn (1992):

$$\left\langle \Delta x^2_{\text{conf}} \right\rangle = C/\log(\eta). \tag{22}$$

The logic behind this equation is not clear, in particular, the effect of a finite instrumental resolution is not taken into account.

Experimental results

Materials and methods

Hydrated samples of horse myoglobin (Sigma M 0630) or chicken egg lysozyme (Sigma L 7651) were prepared after purification by rehydrating lyophilized material with H_2O or D_2O in a controlled humidity environment. The final degree of hydration was determined by weighing, ranging from 0.05 to 0.4 (±0.01) g/g protein. Vitrified myoglobin samples were prepared by dissolving D-exchanged myoglobin in a concentrated D-glucose solution (ChemPur), which was dried under vacuum at 60°C. The resulting glass had the same melting temperature. A typical amount of 300 mg sample was filled in a thin vacuum-tight, flat aluminium cell with 50 mm diameter and 0.5 mm intervall spacing. The samples were measured using the time-of-flight spectrometer IN6 (ILL Grenoble) at a wavelength of 5.1 Å and 100 μeV resolution (FWHM) and the back-scattering spectrometer IN13 (ILL Grenoble) at a wavelength of 2.23 Å. An energy resolution of 8 μeV (FWHW) was achieved. The transmission of the samples was 92%. Multiple scattering corrections were performed for all elastic scans (Settles and Doster 1997). The initial data reduction was performed using standard ILL programs, which correct for incident flux, cell scattering and self-shielding using an angle-dependent slap correction. To compensate for detector efficiency, the data were normalized to a vanadium spectrum, which was also used to determine the instrumental resolution function.

Displacements observed on different time scales Neutron- and Mössbauer-spectroscopy

Figure 4 compares the displacements of the non-exchangeable hydrogens of D_2O-hydrated myoglobin and lysozyme at the same degree of hydration, 0.35 g/g, derived from elastic neutron back-scattering experiments. The second moments were obtained from a cumulant analysis of the scattering function $I_{\text{el}}(Q)$ yielding the low Q limit (Doster and Settles 2005). The zero point vibrations were removed by normalizing to data at 20 K. The resulting vibrational displacements in myoglobin and lysozyme at low temperatures are consistent with those derived from the respective vibrational density of states as shown in Fig. 4 (Settles and Doster 1997). With both proteins, myoglobin and lysozyme a deviation from linear behaviour occurs at 180–200 K. The onset with lysozyme occurs at a slightly lower temperature. A second nonlinear enhancement occurs above 240 K, which is more pronounced for myoglobin than for lysozyme. Below it is shown that this reflects the dynamical transition induced by water-coupled protein motions, which is determined by the ratio $\tau_c(T)/\tau_{\text{res}}$ (Doster et al. 1989). The temperature-dependent displacements thus reveal also differences in internal mobility and protein–water interactions.

In the case of the back-scattering spectrometer IN13 the energy resolution of 7 μeV corresponds to a time window of τ_{res} = 50 ns (Doster et al. 1989; Doster and Settles 2005). A nonlinear onset in the displacements of myoglobin was first recorded with Mössbauer resonance absorption spectroscopy. This method, which monitors the displacements of the heme iron, exhibits a much higher energy resolution than neutron back-scattering. It corresponds to a time window of 141 ns, the nuclear life time of ^{57}Fe (Parak and Formanek 1971; Keller and Debrunner 1980; Parak et al. 1981; Parak and Knapp 1984; Parak and

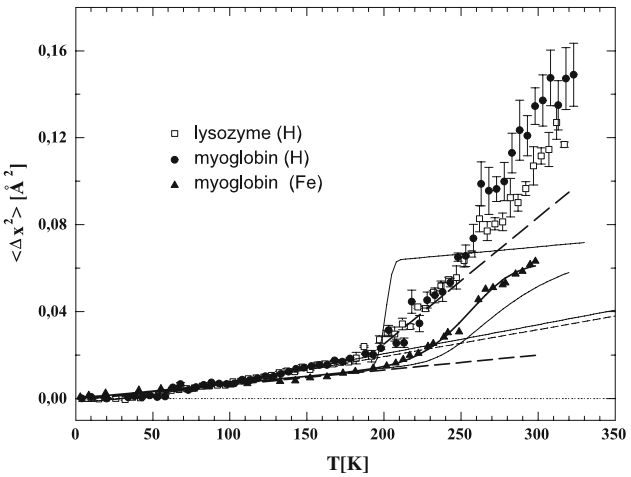

Fig. 4 Mean square displacements of the non-exchangeable hydrogens (H) of D_2O-hydrated myoglobin (*full circles*) and lysozyme (*open squares*) at 0.35 g/g as derived from neutron back-scattering (IN13), *full triangles*: heme–iron displacements derived from Mössbauer absorption spectroscopy of oxy-myoglobin crystals (Parak et al. 1981). The *dashed lines* are drawn to emphasize the onset of the first (180 K) and second (240 K) transition. The *full lines* (myoglobin) and *short dashed lines* (lysozyme) reflect vibrational displacements calculated from the experimental vibrational density of states. The *full lines* are displacements calculated based on the assumption of a resolution-limited process coupled to the reorientation of hydration water for 140 ns and 50 ps resolution time (see text)

Achterhold 2005). In spite of this difference the onset occurs in a similar temperature range, 180–200 K. Moreover, the Mössbauer absorption data refer to a single, effective Q-value of 7.31 $Å^{-1}$, which exceeds the maximal value of the range covered with neutron back-scattering (0.1–5 $Å^{-1}$). The relevant Q^2-values differ thus by at least a factor of two: 50 versus 25 $Å^{-2}$. The published iron displacements thus involve a sizeable extrapolation to $Q \rightarrow$ zero with the additional assumption of a Gaussian displacement distribution valid at all Q-values. The resulting amplitudes thus represent a lower limit to the true values. The heme displacements shown in Fig. 4 are indeed significantly below those observed for the protein hydrogens. Considering the differences in monitor (H vs. Fe), the Q-range, the preparation (hydrated powder versus crystal) and the time-resolution between the two methods, it is striking, that there is a common nonlinear onset near 180–200 K. This coincidence motivated us to introduce the asymmetric two-state model: it predicts a fixed onset temperature independent of the instrumental resolution (Doster et al. 1989). The asymmetric two-state model was invoked also by Keller and Debrunner 1980 to explain the mobility onset of the heme iron near 200 K. Parak et al. (1981; Parak and Knapp 1984) extended this model by suggesting a harmonic envelope potential decorated with traps, the conformational substates. In both models the onset at 200 K is amplitude-driven: the iron moves out of the trap above 200 K and performs a diffusive motion along the harmonic potential. This gives rise to a broad quasi-elastic line with increasing intensity at constant width (Parak and Achterhold 2005). In parallel, the area of the elastic line decreases due to the sum rule, which leads to the recorded increase in the displacements. Also a slight broadening of the elastic line is observed. Experimentally, it is difficult to extract the broad line from the noisy background. The trap model is not fully convincing, since resolution effects are only partially accounted for. It is a mystery, why the time scale of the envelope diffusion always conincides with the Mössbauer window. As early as 1986 we have proposed a resolution-limited onset, triggered by the glass transition of hydration water (Doster et al. 1986). We have further extended this view based on our own Mössbauer studies of myoglobin in 80% sucrose-water (Lichtengegger et al. 1999). Compared to the hydrated crystal an upshift in the onset temperature, (240 K), was observed, due to an increase in the solvent viscosity. The viscosity effect is not compatible with a the substate trap model. We also found for myoglobin in a viscous solution that the central line of the heme-iron spectrum broadens drastically due to center of mass diffusion of the whole protein molecule. Because of the large effective Q-value of 7.3 $Å^{-1}$ the method is sensitvie to very small displacements on a scale of 0.14 Å. On this scale even slow protein diffusion (D) gives rise to a short correlation time, $\tau^{-1} = Q^2\ D$, on a scale of nanoseconds. The increase in line-width of the elastic component varies thus with the solvent viscosity: $D \propto 1/\eta$. However, in addition to an increase in the width, the area of the elastic line decreases, suggesting the existence of faster internal motions. This onset also shifts with the viscosity of the solvent near the protein surface (Kleinert et al. 1998; Lichtengegger et al. 1999).

The onset near 180 K is thus easier to explain by a resolution-limited process. The fit of the heme displacements according to (7), accounting for a Lorentzian resolution function, is shown in Fig. 4. Assuming a single activated relaxation process with constant amplitude fits the iron-displacements quite well and yields an activation energy of 25 (±2) kJ/mol. The correlation time at 200 K is 2 μs and the corresponding total displacement amounts to 0.5 (±0.05) $Å^2$. The common ground between the two methods is the role of hydration water: the relaxational motion of the side-chains and of the heme requires the presence of water (Doster et al. 1989; Doster and Settles 1998; Parak et al. 1987). It was suggested earlier, that the structural relaxation time of the solvent near the protein surface sets the time scale to heme and side-chain displacements (Sing et al. 1981; Doster et al. 1986, 1989; Demmel et al. 1997; Lichtengegger et al. 1999). To model the onset in the case of myoglobin crystals, we use as input the reorientational relaxation time of hydration water as

measured in hydrated met-myoglobin powders with ^{2}H-NMR (Doster and Settles 2005). The reorientation rate displays a super-Arrhenius temperature dependence, where the effective activation energy varies from 20 kJ/mol near room temperature to 180 kJ/mol below 180 K. The resulting onset in Fig. 4 is much more abrupt than the experimental result, but the characteristic temperature of 180 K is correctly predicted. A single water relaxation time and a resolution time of 142 ns were assumed. The neutron scattering experiment with $\tau_{res} = 50$ ps (IN13) leads to an onset temperature of 240 K, where the transition is much less abrupt. The reason is the effective activation energy, which decreases with increasing temperature. Another factor, affecting the width of the transition, is a wide distribution of relaxation times. A perfect fit to the data assuming the Arrhenius law of a single (average) relaxation time is thus not conclusive. Whether the trap model or the dynamics of a water-coupled process provides the correct explanation of the Mössbauer effect, requires further studies of the broad line. But our analysis predicts a water-coupled transition at the neutron scattering time scale near 240 K, which is supported by the data.

Effect of environment and assignment of molecular motions

A quite useful approach to discriminate between different types of molecular motions is to probe their sensitivity to the protein environment. Three extreme environments have been chosen: dehydrated myoglobin, fully D_2O-hydrated myoglobin (0.35 g/g) and myoglobin vitrified in a perdeuterated glucose glass. With these preparations about 90% of the elastic scattering function, probed with the back-scattering spectrometer IN13, derives from the non-exchangeable hydrogens of the protein. The wide Q-range of this spectrometer allows one to identify particular molecular motions according to their spatial characteristics. In our previous work we have shown that with dehydrated proteins only motions related to the onset below 200 K are observed (Doster et al. 1989; Doster and Settles 2005; Doster 2006).

Figure 5 compares elastic scattering functions derived for two dehydrated proteins with the small Q-range spectrmeter HFBS (NIST) by Sokolov et al. (2005) to wide Q-range IN13 data (Doster and Settles 2005). The data are corrected for the vibrational Debye–Waller factor. It is evident, that a fit to the elastic incoherent structure factor (EISF) of methyl group rotation makes only sense with the wide-Q range of IN13. The resulting partial scattering cross-section amounts to 28%, close to the 25% expected from the content of methyl groups. As a second method to identify the spectral contribution of methyl groups is the

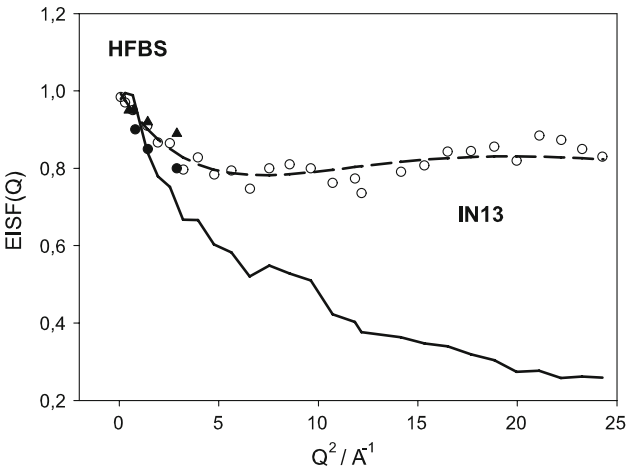

Fig. 5 Elastic scattering function observed with the back-scattering spectrometer HFBS (NIST) of dehydrated lysozyme (*triangles*) in comparison with results obtained with IN13 (ILL) with dehydrated myoglobin corrected for a Gaussian component (*full line*). Also shown is the EISF(Q) of rotational jumps between three states i.e. a methyl group (*dashed line*)

isotopic substitution by CD_3. With perdeuterated bacteriorhodopsion the initial transition at 150–180 K is indeed absent (Zaccai 2000), which supports the above assignment.

Figure 6 shows a decomposition of vibrational and diffusive displacements depending on the protein environment. The temperature dependence of the harmonic components can be characterized by a hyperbolic cotangent function. In the glucose glass slightly lower amplitudes are observed than with dry myoglobin. The low-temperature onset of diffusive motions in all three environments occurs at about 150 K also in the vitrified case. This result

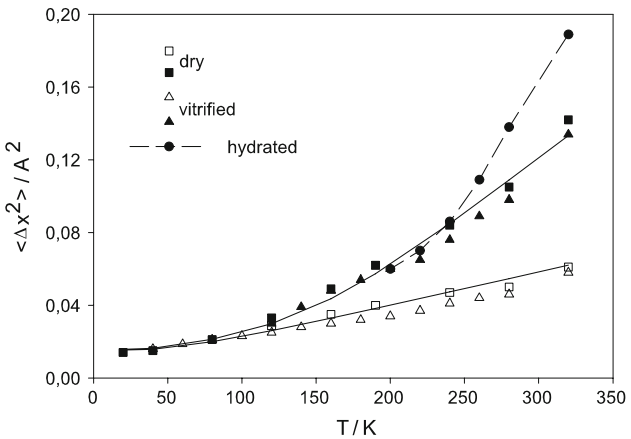

Fig. 6 Total and vibrational mean square displacements (IN13) derived from a cumulant analysis of the elastic scattering function of D_2O-hydrated myoglobin, $h = 0.35$ (*full dots*) (Doster et al. 1989), dehydrated myoglobin (*squares*) and glucose-vitrified myoglobin (*triangles*). The *full lines* in the dry case were derived assuming the EISF and the correlation time for methyl group rotation

demonstrates the existence of solvent-decoupled molecular motions in proteins. The solid line represents a calculation assuming rotational transitions of methyl groups as the main process in dry or vitrified myoglobin, fits the data quite well without using adjustable parameters. The double-well model was thus extended to three wells of equal energy. The onset reflects the jump-time of methyl group rotation following an Arrhenius law with an average activation energy of 10.5 kJ/mol (Doster and Settles 2005; Doster 2005, 2006). Obviously methyl group torsional transitions can occur in the protein interiour irrespective of the environment. The second onset temperature at 240 K was assiged in 1989 to a dynamical transition of vitrified protein–hydration water (Doster et al. 1989). The corresponding displacement distribution is Gaussian and could be interpreted in terms of small-scale motions in a harmonic potential well (Doster and Settles 2005). As will be shown below, although a harmonic envelope potential with traps would fit the data, the onset at 240 K is not induced by enhanced motional amplitudes.

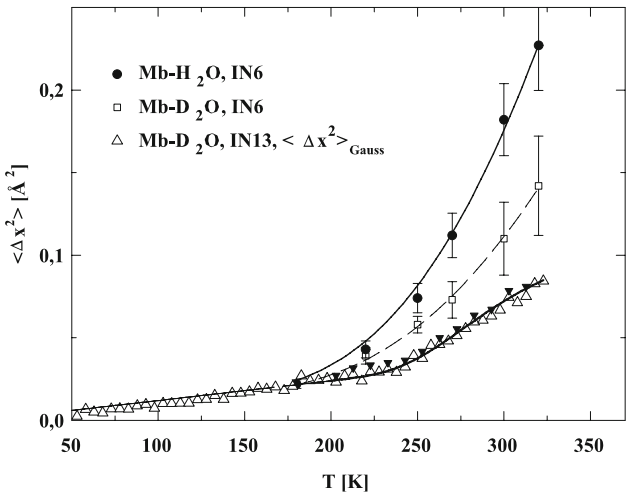

Fig. 7 Mean square displacements, IN 6: D_2O–hydrated myoglobin and hydration water (H_2O–hydrated myoglobin) and IN 13 of D_2O- (*open triangles*) and H_2O–hydrated (*full trianglses*) myoglobin (0.35 g/g): Gaussian component with contribution of methyl groups removed. The *full lines* represent the fits to an asymmetric two-state model (IN6) and to a water-coupled process, limited by the instrumental resolution (IN13)

Hydrogen bond fluctuations as a precursor of the dynamical transition

From these considerations it seems to follow that the onset of relaxational displacements is generally related to the instrumental resolution function. However, in previous work with hydrated myoglobin we found that the high-frequency tail of the time-of-flight spectrum increases exponentially with temperature at nearly constant relaxation rate. This feature was assigned to an amplitude increase due to fast hydrogen bond fluctuations between open and closed states. This process is appropriately described by an asymmetric two-well model (Doster et al. 1989; Demmel et al. 1997; Doster and Settles 1998). This interpretation is further supported by molecular dynamic simulations of water in hydrated proteins (Tarek and Tobias 2002a, 2002b). Fast hydrogen bond fluctuations are more easily observed with the low resolution, high-flux time-of-flight spectrometer (IN6) than with high-resolution back-scattering spectroscopy. In the back-scattering time window methyl group rotation dominates, which makes it difficult to discriminate this process from small scale hydrogen bond fluctuations. The time window of IN6 at 100 μeV (FWHM) covers about 15 ps. Such 15 ps TOF-displacements with H_2O- and D_2O hydrated myoglobin (0.35 g/g) are displayed in Fig. 7. The displacements in both systems increase in parallel with a common onset at 180–200 K. In the H_2-O system mainly water is observed, because of the large cross-section (60%) and the large motional amplitude of water relative to structural fluctuations. In the D_2O system protein fluctuations with smaller amplitudes are observed. The common temperature dependence suggests a common cause of protein- and water-displacements. Note that this transition is unrelated to methyl group dynamics, since the respective correlation time at 180 K ranges near 1 ns. This time scale is far outside the spectral window of IN 6 (15 ps) (Doster 2006). The onset at 180 K correlates with the intensity increase of the high frequency spectrum suggesting a fast amplitude-controlled process similar in nature to open and closed transitions of hydrogen bonds. A similar mechanism has been proposed in a slightly different context to explain the temperature dependence of the IR amide bands of myoglobin in mixed solvents (Demmel et al. 1997). The resulting values for the enthalpy and entropy differences for H_2O are close to the numbers derived in 1989 (Doster et al. 1989): $\Delta H \approx 14\ (\pm 2)$ kJ/mol and for the entropy $\Delta S/R \approx 3.5\ (\pm 0.3)$. The total conformational displacements range near 1.7 (±0.1) Å. In the case of the D_2O-hydrated sample the same enthalpy and entropy differences are obtained, but the respective conformational displacements are somewhat smaller, 1(± 0.1) Å.

The same two samples with H_2O and D_2O hydration were investigated on a 50 ps time scale using back-scattering. The resulting displacements, the contribution of the methyl groups was subtracted, are shown in Fig. 7. Both, protein- and water-displacements are similar in magnitude and exhibit the same temperature dependence. The transition temperature is up-shifted to 240 K in spite of a longer observation time (50 vs. 15 ps).

In contrast, since the TOF experiments are sensitive to much faster motions than back-scattering, a down-shift is

to be expected. This discrepancy supports our conjecture, that with TOF-spctroscopy indeed faster dynamic components contribute to the onset than with back-scattering. Fast H-bond fluctuations can be considered as the precursor (or β-process) of the slow structural (or α-) process. The latter should be closely related to reorientation and diffusion of water near the protein surface. The reorientational motion of water (D_2O) near the surface of myoglobin was determined using ^{2}H-NMR (Doster and Settles 2005). The method probes the reorientational relaxation of the O–D vector. A super-Arrhenius temperature dependence with the following parameters was detected: A^*/R = 460 ($\pm$40) K, T_0 = 167 ($\pm$5) K and log (τ_0/ps) = $-$0.024 ($\pm$0.01). Using the parameters for τ_c (T) of hydration water and assuming resolution-limited displacements parametrized by (7) leads to the solid line in Fig. 7. The nearly perfect agreement of data and fit supports the idea that the dynamical transition at 240 K is created by the crossing of two characteristic times: The instrumental resolution time of 50 ps and a strongly temperature dependent reorientational rate of protein–adsorbed water. This result further suggests, that the water-induced transition observed with hydrated myoglobin at 240 K on a 50 ps time scale is closely related to the onset of heme-displacements, which occurs at 200 K since relevant instrumental time scale is 3,000 times longer.

Conclusions

The main goal of low temperature studies, separating the dynamical components of protein structural fluctuations and their coupling to the solvent, has been achieved. We can now account for the molecular displacements, observed with elastic neutron scattering in hydrated protein powders, on a quantitative basis: (1) the vibrational mean square displacements follow from the distribution of low frequency vibrational states, (2) the nonlinear enhancement of motional amplitudes starting above 150 K can be explained by rotational transitions of methyl side-chains, (3) fast H-bond fluctuations contribute to the high frequency spectrum of H_2O- and D_2O-hydrated proteins and finally (4) small scale librational motions of side-chains are coupled to rotational diffusion of water near the protein surface. Not any deviation from a linear temperature-dependence of the squared displacements reflects a dynamical transition. The transition was initially assigned to a resolution-limited process on a 50 ps time scale with displacements emerging at 240 K. The term “transition” implies a drastic variation of the corresponding relaxation rates within a narrow temperature range. This is one of the characteristic features of the glass transition, which is a kinetic and not a thermodynamic phenomenon. The rate of the corresponding structural α-process varies in super-Arrhenius fashion, when a critical temperature is approached. On a logarithmic scale, the structural relaxation time varies smoothly with temperature. This apparent continuity on a log-scale has led to the misconception of discarding the concept of a transition at all. However physical quantities like molecular displacements, specific heat and thermal expansion exhibit an abrupt onset on a linear temperature scale at the glass transition temperature. The onset at 240 K can thus be interpreted as the glass temperature with respect to a 50 ps time scale. Liquid behaviour implies long-range diffusion, which is arrested at the glass transition. Since water near the protein surface can perform long range diffusion, which is arrested near 200 K (Doster and Settles 2005), it shows liquid behaviour above 200 K and glassy behaviour below. The slow α-process can be associated with the elementary step of diffusion. Hydration- and bulk-water thus differ essentially in the magnitude of the diffusion coefficient and the rate of crystallization. β-processes in contrast, involve localized librational motions, which can act as a precursor of long-range diffusion. Hydrogen-bond fluctuations would thus classify as β-processes. Contrasting suggestions by Frauenfelder et al. are misleading (Fenimore et al. 2005), since diffusion within the hydration shell is ignored. The combined results suggest that the onset, observed in the range between 150 and 200 K for dehydrated as well as with hydrated or vitrified proteins reflects both, resolution limited torsional motions as well as amplitude limited hydrogen bond fluctuations. In the language of polymer dynamics torsional transitions of side-chains could be classified as γ-processes. To unravel the multi-component features of protein dynamics with neutron scattering, elastic scattering profiles have to be complemented by spectral information. Extended-range spectra were already presented in the original work in 1989 (Doster et al. 1989). Models have to be designed, which predict the complete neutron scattering spectrum and not just the elastic fraction. The forces constant model does not account for resolution effects and deviations from a harmonic potential. The original picture of a well-defined energy landscape controlling protein dynamics does not account for the solvent (Fenimore et al. 2005). The liquid acts as a plastiziser modulating the barriers of the landscape. The dynamical transition thus leads from a rigid landscape to a seascape, where barriers are less relevant to motion than the configurational entropy.

Acknowledgments This work was supported by a grant of the Deutsche Forschungsgemeinschaft within the SFB 533, light-induced processes in biopolymers. Excellent technical support by the instrument responsibles including the Institut Laue Langevin and numerous discussions with Prof. Wolfgang Götze are gratefully acknowledged. The NMR experiments were performed by Prof. Franz Fujara.

References

Becker T, Smith J (2003) Energy resolution and dynamical heterogeneity effects on elastic incoherent neutron scattering from molecular systems. Phys Rev E 67:021904-1-8

Becker T, Hayward JA, Finney JL, Daniel RM, Smith J (2004) Neutron frequency windows and the protein dynamical transition. Biophys J 87:1436–1444

Bicout DJ, Zaccai G (2001) Protein flexibility from the dynamical transition, a force constant analyis. Biophys J 80:115-1123-8

Buchenau U, Zorn R (1992) A relation between fast and slow motions in glassy and liquid selenium. Europhys Lett 18:523–528

Cornicchi E, Onori G, Paciaroni A (2005) Picosecond time scale fluctuations of proteins in glassy matrices: the role of viscosity. Phys Rev Lett 95:158104-1-4

Daniel RM, Finney JL, Reat V, Dunn R, Ferrand M, Smith J (1999) Enzyme dynamics and activity, the time scale dependence of dynamical transitions. Biophys J 77:2184–219

Demmel F, Doster W, Petry W, Schulte A (1997) Vibrational frequencies as a probe of hydrogen bonds: thermal expansion and glass transition of myoglobin in mixed solvents. Eur Biophys J 26:327–335

Doster W (2005) Brownian oscillator analysis of molecular motions in biomolecules. In: Fitter J, Gutberlet T, Katsaras J (eds) Neutron scattering in biology. Springer series biological and medical physics, biomedical engineering, pp 461–482

Doster W (2006) Dynamic structural distributions in proteins. Physica B 385–386:831–834

Doster W, Settles M (1998) Dynamical transition of proteins, the role of hydrogen bonds. In: Bellissent-Funel M-C (ed) Hydration processes in biology (Les Houches lectures). IOS Press, Amsterdam, pp 177–190

Doster W, Settles M (2005) Protein–water displacement distributions. Biochim Biophys Act 1749:173–186

Doster W, Lüscher E, Bachleitner A, Dunau R, Hiebl M (1986) Thermal properties of water in myoglobin crystals and solutions at subzero temperatures. Biophys J 50:213–219

Doster W, Cusack S, Petry W (1989) Dynamical transition of myoglobin revealed by inelastic neutron scattering. Nature 337:754–756

Doster W, Cusack S, Petry W (1990) Dynamic instability of liquid-like motions in proteins. Phys Rev Lett 65:1083–1086

Doster W, Diehl M, Petry W, Ferrand M (2001) Elastic resolution spectroscopy: a method to study molecular motions in small biological samples. Physica B 301:65–68

Doster W, Diehl M, Gebhardt R, Lechner RE, Pieper J (2003) Time-of-flight elastic resolution spectroscopy: time domain analysis of weakly scattering samples. Chem Phys 292:487–494

Fenimore P W, Frauenfelder H, McMahon BH, Young RD (2005) Proteins are paradigms of stochastic complexity. Physica A 351:1–13

Ferrand M, Dianoux AJ, Petry W, Zaccai G (1993) Thermal motions and function of bacteriorhodopsin in purple membranes: effects of temperature and hydration studied by neutron scattering. Proc Natl Acad Sci USA 90:9668–9672

Fitter J, Lechner RE, Dencher NA (1997) Picosecond molecular motions in bacteriorhodopsin from neutron scattering. Biophys J 73:2126–2137

Gabel F (2005) Protein dynamics in solution and powder measured by incoherent elastic neutron scattering. Eur Biophys J 34:1–12

Gabel F, Bicout D, Lehnert U, Tehei M, Weik M, Zaccai G (2002) Protein dynamics, studied by neutron scattering. Q Rev Biophys 35:1–32

Götze W, Sjögren L (2005) Relaxation processes in supercooled liquids. Rep Prog Phys 55:241–376

Hayward JA, Finney JL, Daniel RM, Smith JC (2003) Molecular dynamics decomposition of temperature-dependent elastic neutron scattering by a protein solution. Biophys J 85:679–685

Keller H, Debrunner P (1980) Evidence for conformational and diffusional mean square displacements in frozen aqueous solution of oxy-myoglobin. Phys Rev Lett 45:68–71

Kleinert Th, Doster W, Leyser H, Petry W, Schwarz V, Settles M (1998) Solvent composition and viscosity effects on the kinetics of CO-binding to horse myoglobin. Biochem 37:717–733

Kurkal V, Daniel RM, Finney JL, Tehei M, Dunn RV, Smith J (2005) Enzyme activity and flexibility at very low hydration. Biophys J 89:1282–11287

Lichtengegger H, Doster W, Kleinert T, Birk A, Sepiol B, Vogl G (1999) Heme-solvent coupling, a Mössbauer study of myoglobin in sucrose. Biophys J 76:414–422

Magazu S, Maisano G, Migliardo F, Mondelli C (2004) Mean square displacement relationship in bioprotectant systems by elastic neutron scattering. Biophys J 86:3241–3249

Nakagawa H, Kmikubo I, Kanaya T, Kataoka M (2004) Protein dynamical heterogeneity derived from neutron incoherent elastic scattering. J Phys Soc Jpn 73:491–495

Paciaroni A, Cornicchi E, De Francesco A, Marconi M, Onori G (2006) Conditioning action of the environment on the protein dynamics studied through elastic neutron scattering. Eur Biophys J 35(7):591–599

Parak F, Achterhold K (2005) Protein dynamics on different timescales. J Phys Chem Solids 66:2257–2262

Parak F, Formanek H (1971) Untersuchung des Schwingungsanteils und des Kristallgitterfehleranteils des Temperaturfaktors in Myoglobin durch Vergleich von Mössbauerabsorptionsmessungen mit Röntgenstrukturdaten. Acta Crystallogr A 27:573–578

Parak F, Knapp EW (1984) A consistent picture of protein dynamics. PNAS USA 81:7088–7092

Parak F, Frovlov EN, Mössbauer RL, Goldanskij VI (1981) Dynamcis of metmyoglobin investigated by nuclear gamma-resonance absorption. J Mol Biol 145:237–249

Parak F, Fischer M, Graffweg E Formanek, H (1987) Distributions and fluctuations of protein structures investigated by X-ray analysis and Mössbauer spectroscopy. In: Clementi E, Chin S (eds) Structure and dynamics of nucleic acids, proteins and membranes. Plenum Press, New York, pp 139–148

Reat V, Zaccai G, Pfister C, Ferrand M (1997) Functional dynamics in purpel membrane. In: Cusack S, Büttner H, Ferrand M, Langan P, Timmins P (eds) Biological macromolecular dynamics. Adenine Press, New York, pp 117–122

Reat V, Dunn R, Ferrand M, Finney JL, Daniel RM, Smith JC (2000) Solvent dependence of dynamic transitions in protein solutions. Proc Natl Acad Sci USA 97:9961–9966

Roh JH, Novikov VN, Gregory RB, Curtis JE, Chowduri Z, Sokolov AP (2005) Onset of unharmonicity in protein dynamics. Phys Rev Lett 95:038101

Russo D, Perez J, Zanotti JM, Desmadril M, Durand D (2002) Dynamic transition associated with the thermal denaturation of a small beta protein. Biophys J 83:2792–2800

Sartor G, Mayer E, Johari GP (1994) Calorimetric studies of the kinetic unfreezing of molecular motions in hydrated lysozyme, hemoglobin and myoglobin. Biophys J 66:249–258

Serdyuk IN, Zaccai NR, Zaccai G (2007) Methods in molecular biophysics. Cambridge University Press, London, p 957

Settles M, Doster W (1997) Iterative calculation of the vibrational density of states from incoherent neutron scattering data with the account of double scattering. In: Buettner H, Cusack S, Ferrand M, Lagan P, Timmins P (eds) Biological macromolecular dynamics. Adenine Press, New York, pp 3–9. ISBN 0-940030-49-7

Sing GP, Parak F, Hunklinger S, Dransfeld K (1981) Role of adsorbed water in the dynamics of metmyoglobin. Phys Rev Lett 47:685–688

Smith J (1991) Protein Dynamics, a comparison of simulations with inelastic neutron scattering experiments. Q Rev Biophys 24:227–291

Smith DJ, Ferrand M, Hery S, Dunn RJ, Finney JL (1998) Enzyme activity below the dynamical transition. Biophys J 75:2504–2507

Tarek M, Tobias D (2002) Single particle and collective dynamics of protein hydration water. Phys Rev Lett 89:13801–13804

Tarek M, Tobias T (2002) The role of protein–water hydrogen bonds in the dynamical transition of proteins. Phys Rev Lett 88:381011–381013

Tehei M, Madern D, Franzetti B, Zaccai G (2005) Neutron scattering reveals the dynamic basis of protein adaption to extreme temperature. J Bio Chem 280:40974–40979

Tehei M, Smith JC, Monk C, Ollivier J, Oettl M, Kurkal V, Finney JL, Daniel RM (2006a) Dynamics of immobilized and native *E. coli* dihhydrofolate reductase by quasi-elastic neutron scattering. Biophys J 90:1090–1097

Tehei M, Daniel R, Zaccai G (2006b) Fundamental and biotechnological application of neutron scattering measurements for macromolecular dynamics. Eur Biophys J 35:551–558

Tournier AL, Smith JC (2003) Principal components of the protein dynamical transition. Phys Rev Lett 91(20):208106-1–208106-4

Tournier AL, Xu J, Smith JC (2003) Solvent caging of internal motions in myoglobin at low temperatures. Phys Chem Commun 6(2):6–8

Tsai AM, Neumann DA, Bell LN (2000) Molecular dynamics of solid-state lysozyme as affected by glycerol and water, a neutron scattering study. Biophys J 79:2728–2732

Zaccai J (2000) How soft is a protein? A protein force constant measured by neutron scattering. Science 288:1604–1607